Spin-density-wave effects on the vibrational anharmonicity of acoustic phonons in Cr-Ir alloy single crystals

1998 J. Phys.: Condens. Matter 10 11731

(http://iopscience.iop.org/0953-8984/10/50/012)

J. Phys.: Condens. Matter **10** (1998) 11731–11742. Printed in the UK PII: S0953-8984(98)97495-1

Spin-density-wave effects on the vibrational anharmonicity of acoustic phonons in Cr–Ir alloy single crystals

J Martynova, H L Alberts and P Smit

Department of Physics, Rand Afrikaans University, PO Box 524, Auckland Park, Johannesburg 2006, South Africa

Received 14 September 1998

Abstract. Measurements are reported of the dependences on hydrostatic pressure (p) of the elastic constants (c_{ij}) of Cr–Ir alloy single crystals containing 0.07 at.% and 0.20 at.% Ir. For the former concentration the alloy exhibits a transition from an incommensurate (I) spin-density-wave (SDW) to a paramagnetic state at the Néel temperature (T_N). $\mathrm{d}c_{ij}/\mathrm{d}p$ was studied as a function of temperature through T_N. The concentration of the $Cr_{0.998}Ir_{0.002}$ crystal is larger than the triple-point concentration on the Cr–Ir magnetic phase diagram and for this crystal there appears a phase transition from an ISDW to a commensurate (C) SDW at T_{IC}. $\mathrm{d}c_{ij}/\mathrm{d}p$ was measured for this crystal as a function of temperature through T_{IC}. The acoustic mode Grüneisen parameters were calculated for the two crystals as a function of temperature through T_N (for $Cr_{0.9993}Ir_{0.0007}$) and through T_{IC} (for $Cr_{0.998}Ir_{0.002}$). Large negative Grüneisen parameters are observed in the ISDW and CSDW phases of $Cr_{0.998}Ir_{0.002}$. The results indicate stronger magnetoelastic interactions in the CSDW than in the ISDW phase of this crystal. It is shown that the strong magnetoelastic coupling in the ISDW and CSDW antiferromagnetic phases of the Cr–Ir system takes mainly place through volume effects.

1. Introduction

Chromium and its dilute alloys possess extraordinary antiferromagnetic properties [1]. They are spin-density-wave (SDW) itinerant-electron antiferromagnetic materials in which the magnetic properties are strongly volume dependent [2], particularly the magnetoelastic properties, which show unusual effects under the application of hydrostatic pressure [3]. This strong volume dependence is at present not well understood [2]. Dilute alloys of Cr with the group-8 non-magnetic transition metals, Ru, Ir, Pd, Rh and Pt, are of particular interest in this regard, as it was recently observed [3] that the acoustic mode vibrational anharmonicity, determined by the pressure dependence of the elastic constants, of a Cr+0.3 at.% Ru crystal is strongly affected by the presence of the SDW. This crystal is the only one to date for which vibrational anharmonic effects have been studied through an incommensurate–commensurate (I–C) SDW phase transition.

The addition of only a small amount of a group-8 non-magnetic transition metal to Cr changes the incommensurate (I) SDW state of pure Cr to a commensurate (C) SDW state. For such dilute Cr alloys there exists a triple-point concentration (x_t) on the magnetic phase diagram such that for $x < x_t$ the alloy remains in the ISDW phase at all temperatures below the Néel point (T_N) while both ISDW and CSDW phases, with an ISDW–CSDW phase transition at $T = T_{IC}$, are found for $T < T_N$ in alloys with $x > x_t$.

Unusual anharmonic effects were observed [3] in a Cr + 0.3 at.% Ru crystal. The acoustic mode Grüneisen parameters, which quantify the vibrational anharmonicity, for

0953-8984/98/5011731+12$19.50

longitudinal modes in this alloy are negative and relatively large, which is unusual, in both the ISDW and CSDW phases, being larger in magnitude in the CSDW phase. The shear mode Grüneisen parameters, on the other hand, behave normally in both SDW phases, being small and positive. The results show strong coupling of the SDW to the longitudinal mode acoustic phonons. Coupling to the shear mode phonons is relatively weak.

Negative acoustic mode Grüneisen parameters were recently also observed [4, 5] in itinerant-electron ferromagnetic Invar materials. In the ferromagnetic case an attempt was made [6] to understand the reason for these negative parameters by carrying out a simple model calculation for the thermal expansion coefficient using a jellium-like model. It appears that negative Grüneisen parameters are brought about by a situation where the phonon contribution to the thermal expansion dominates over that of the electrons. A theoretical explanation for negative Grüneisen parameters in itinerant antiferromagnetic Cr alloys has, however, not yet been attempted.

To investigate the situation further in the itinerant antiferromagnetic case, we report here a study of the acoustic mode vibrational anharmonicity of the Cr–Ir alloy system. Ir, like Ru, is a member of the group of alloys with group-8 non-magnetic transition metals. The present study on the Cr–Ir system should verify whether the unusual anharmonic effects observed around the ISDW–CSDW phase transition in the Cr + 0.3 at.% Ru alloy are more general phenomena of Cr alloy systems with group-8 non-magnetic transition metals. Two Cr–Ir alloy single crystals were studied. One, Cr + 0.20 at.% Ir, has $x > x_t$ and displays, like Cr + 0.3 at.% Ru, a CSDW–paramagnetic (P) Néel transition as well as ISDW–CSDW phase transition. For the other Cr–Ir alloy (Cr + 0.07 at.% Ir), $x < x_t$, giving an ISDW–P Néel transition at T_N without any ISDW–CSDW transition at $T < T_N$. This allows for studying the vibrational mode anharmonicity, through both an ISDW–P and CSDW–P phase transition, as well as through an ISDW–CSDW one, of a system of alloys of Cr with group-8 non-magnetic transition metals. These two alloys, furthermore, make it possible to study and to compare anharmonic effects in the ISDW phases for both $x < x_t$ and $x > x_t$ of the same alloy system.

2. Experimental procedure

We managed to grow good-quality Cr + 0.07 at.% Ir and Cr + 0.20 at.% Ir alloy single crystals by a floating-zone technique using RF heating in a pure argon atmosphere. These were the same crystals as were used in a previous study [7] on the magnetoelastic properties at atmospheric pressure. Details of the experimental techniques used to obtain the pressure derivatives of the elastic constants from ultrasonic wave velocity measurements at constant temperature have been described [8] previously. The same methods were used to obtain $\mathrm{d}c_{11}/\mathrm{d}p$, $\mathrm{d}c_{44}/\mathrm{d}p$ and $\mathrm{d}c'/\mathrm{d}p$, where $c' = \frac{1}{2}(c_{11} - c_{12})$, for the two Cr–Ir crystals.

3. Results

3.1. Ultrasonic wave velocities as a function of applied pressure at different constant temperatures

It is usual [3, 8, 9] to present the pressure dependence of the ultrasonic wave velocities for the different propagation modes in terms of the relative change in natural velocity, $\Delta W/W_0$. Here $\Delta W/W_0 = (W_p/W_0) - 1$, where W_0 is the natural velocity at $p = 0$ and W_p that at pressure p, both measured at the same constant temperature. The natural velocity, W, is defined [10] as the path length at zero pressure divided by the transit time at pressure p.

In a typical non-magnetic Cr alloy, like Cr+5 at.% V which remains paramagnetic at all $T > 0$ K [1], $\Delta W/W_0$ increases [11] slightly with increasing pressure. For Cr + 5 at.% V, $\Delta W/W_0$ increases [11] linearly by about 1% GPa^{-1} for [100] longitudinal mode wave propagation while it increases by about 0.5% GPa^{-1} for shear mode wave propagation in the [100] direction.

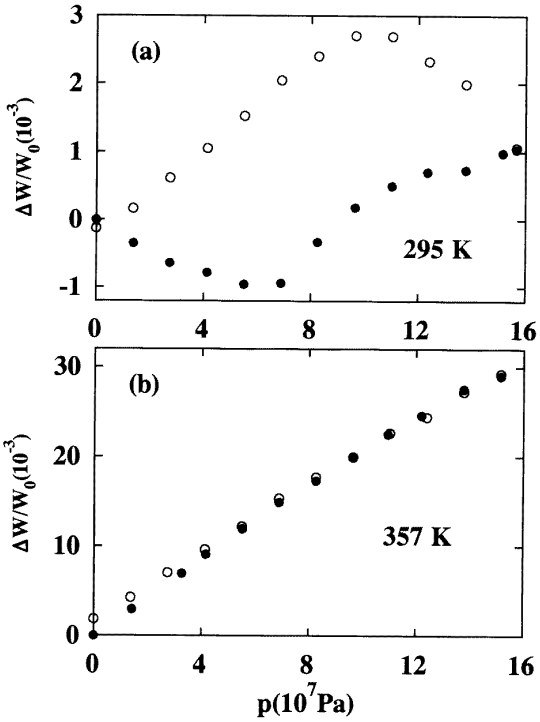

Figure 1. $\Delta W/W_0$, the relative change in natural velocity, for the c_{11} longitudinal wave propagation mode for Cr + 0.07 at.% Ir as a function of pressure at constant temperatures of (*a*) $T = 295$ K $< T_N$ and (*b*) $T = 357$ K $> T_N$. Filled symbols are used for increasing-pressure runs and open ones for decreasing-pressure runs.

The Néel temperature for the Cr+0.07 at.% Ir crystal is [7] $T_N = 324$ K at atmospheric pressure. $\Delta W/W_0$ as a function of pressure at $T < T_N$ for the c_{11} longitudinal wave propagation mode of this crystal behaves anomalously. The $\Delta W/W_0$–p curves at $T < T_N$ for the c_{11} propagation mode of Cr + 0.07 at.% Ir are non-linear, with hysteresis effects, on increasing and decreasing the pressure, as shown by the typical example of figure 1(*a*) at a constant temperature of 295 K. For $T > T_N$, $\Delta W/W_0$ varies nearly linearly with pressure for the c_{11}-mode without any hysteresis effects as shown by the typical example of figure 1(*b*) at 357 K. The slope of the $\Delta W/W_0$–p curves in the paramagnetic phase at $T > T_N$ for this mode of Cr + 0.07 at.% Ir, up to the highest temperature (370 K) of the measurements, is however abnormally high. It is about 20% GPa^{-1}, compared to about 1% GPa^{-1} for the same mode of the paramagnetic Cr + 5 at.% V alloy. Due to the fact that $\Delta W/W_0$–p for longitudinal mode wave propagation at $T < T_N$ for the Cr + 0.07 at.% Ir crystal shows hysteresis effects (figure 1(*a*)), the acoustic mode Grüneisen parameters could not be obtained meaningfully from the measurements of the pressure dependence of the ultrasonic wave velocities of this crystal in its ISDW phase. At $T > T_N$, $\Delta W/W_0$–p curves for

the c_{11}-mode as well as for the c_{44} and c' shear propagation modes were observed to be roughly linear, without hysteresis effects, except for T very close to T_N, allowing for a determination of the Grüneisen parameters at $T > T_N$ for the Cr+0.07 at.% Ir crystal. This will be discussed in the next section.

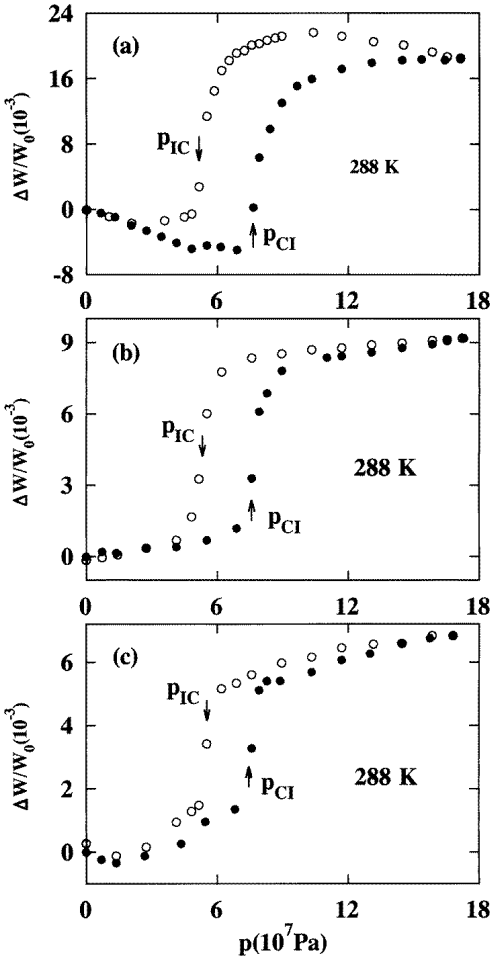

Figure 2. $\Delta W/W_0$, the relative change in natural velocity, for Cr + 0.20 at.% Ir as a function of pressure at a constant temperature of 288 K. Panel (*a*) is for the c_{11} longitudinal wave propagation mode while panels (*b*) and (*c*) are, respectively, for the c_{44} and c' shear wave propagation modes. p_{IC} and p_{CI} are, respectively, the critical pressures for inducing of the I–C and C–I SDW phase transitions. Filled symbols are used for increasing-pressure runs and open ones for decreasing-pressure runs.

For the Cr+0.20 at.% Ir crystal the ISDW–CSDW transition temperature (on heating) is [7] $T_{IC} = 272$ K and the CSDW–ISDW transition temperature (on cooling) is $T_{CI} = 255$ K at atmospheric pressure. The Néel temperature of this crystal at atmospheric pressure is [7] $T_N = 367$ K. $\Delta W/W_0$–p curves were measured for this crystal for longitudinal and shear propagation modes at ten different fixed temperatures in the temperature range from 271 to 360 K. The behaviour of these curves is anomalous at all temperatures. Three examples, for the c_{11}-, c_{44}- and c'-modes, are shown in figure 2 for a constant temperature of 288 K,

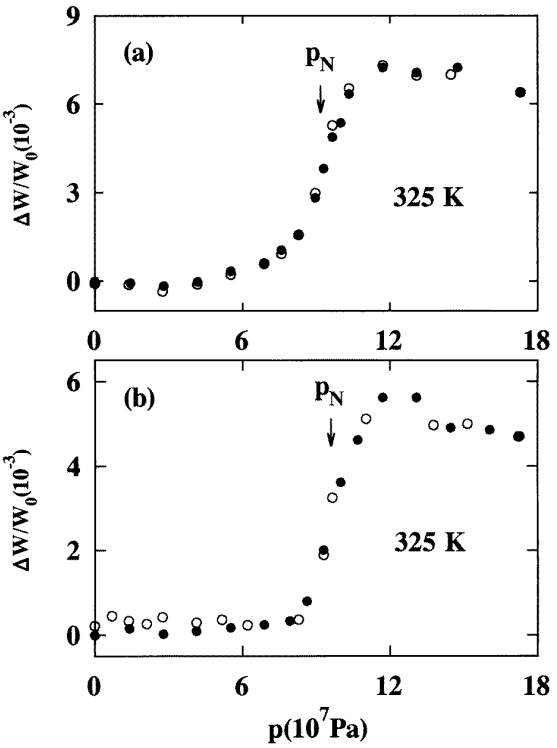

Figure 3. $\Delta W/W_0$, the relative change in natural velocity, for Cr + 0.20 at.% Ir as a function of pressure at a constant temperature of 325 K. Panels (*a*) and (*b*) are, respectively, for the c_{44} and c' shear wave propagation modes. p_N is the critical pressure for inducing of the CSDW–P Néel transition. Filled symbols are used for increasing-pressure runs and open ones for decreasing-pressure runs.

which is close to the I–C and C–I transition temperatures. Figure 3 shows as an example a $\Delta W/W_0$–p curve for the c_{44} shear mode propagation at 325 K, which is relatively far away from T_{IC} and T_{CI}, for this crystal.

For $T < 306$ K the $\Delta W/W_0$–p curves for the c_{11}-, c_{44}- and c'-modes of the Cr + 0.20 at.% Ir crystal are similar to those of the examples in figure 2. They all show a hysteretic transition at a critical pressure p_{CI} on increasing the pressure and at p_{IC} on decreasing it. These pressures were taken at the inflection points of the sharp rises in figure 2 and are ascribed to the applied pressures that induce a CSDW–ISDW transition (p_{CI}) or an ISDW–CSDW transition (p_{IC}). The hysteresis width observed in figure 2 decreases with increasing temperature and disappears around 306 K.

For $T > 306$ K the $\Delta W/W_0$–p curves for the c_{44}- and c'-modes of the Cr+0.20 at.% Ir crystal are similar to the examples of figure 3. They all show a non-hysteretic transition at a critical pressure p_N, which is ascribed to the pressure-induced CSDW–P Néel transition. Due to high ultrasonic attenuation for longitudinal waves at $T > 306$ K in the Cr + 0.20 at.% Ir crystal that increases with increasing pressure, we could not obtain $\Delta W/W_0$ for the c_{11} propagation mode to high enough pressures at $T > 306$ K to observe the CSDW–P Néel transition under applied pressure for the c_{11}-mode. For this mode, pressure runs could only be carried out successfully up to 333 K and 0.06 GPa. The results are

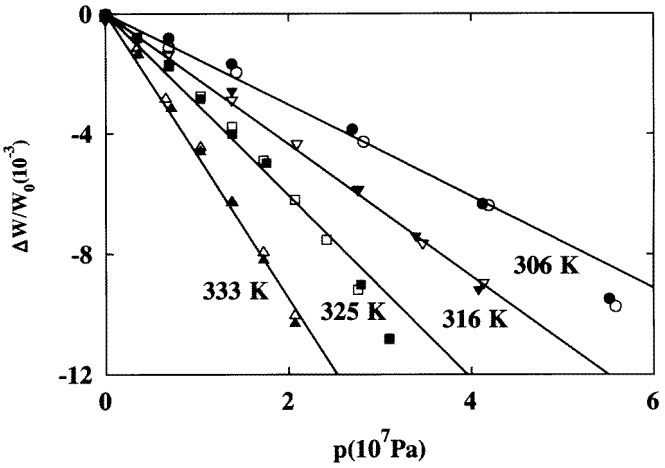

Figure 4. The pressure dependence of $\Delta W/W_0$, the relative change in natural velocity, for the c_{11} longitudinal wave propagation mode of Cr + 0.02 at.% Ir at constant temperatures of 306 K, 316 K, 325 K and 333 K.

shown in figure 4, which shows a nearly linear, relatively sharp, decrease of $\Delta W/W_0$ with increasing pressure at $T > 306$ K.

3.2. Hydrostatic pressure derivatives of the second-order elastic constants

The pressure derivatives, $(\partial c_{ij}/\partial p)_{p=0}$, of the adiabatic second-order elastic stiffness tensor components, c_{11}, c_{44} and c', of Cr+0.20 at.% Ir and Cr+0.07 at.% Ir were determined from the ultrasonic wave velocity measurements as a function of pressure for each propagation mode, by using the relation [10]

$$\left(\frac{\partial c_{ij}}{\partial p}\right)_{p=0} = (c_{ij})_{p=0}\left[2\frac{\partial W/\partial p}{W_0} + \frac{1}{3B}\right]_{p=0} \tag{1}$$

where $B = \frac{1}{3}(c_{11} + 2c_{12})$ is the bulk modulus.

The measurements through p_{IC}, p_{CI} and p_N of the Cr+0.2 at.% Ir crystal, allow for the determination of $(\partial c_{ij}/\partial p)_{p=0}$ in the CSDW as well as in the pressure-induced ISDW and P phases of this crystal. In the case of Cr+0.20 at.% Ir only $(\partial c_{44}/\partial p)_{p=0}$ and $(\partial c'/\partial p)_{p=0}$ could be determined in the pressure-induced (at $T < T_N$) paramagnetic phase but not $(\partial c_{11}/\partial p)_{p=0}$—the reason being the very high ultrasonic attenuation for longitudinal wave propagation in this crystal at $T > 306$ K. For the Cr + 0.07 at.% Ir crystal, $(\partial c_{ij}/\partial p)_{p=0}$ was only determined in its P phase at $T > T_N$ due, as explained previously, to the hysteretic behaviour of the $\Delta W/W_0$–p curves at $T < T_N$.

Figure 5 shows $(\partial c_{ij}/\partial p)_{p=0}$ as a function of temperature for the two crystals. The experimental error in $(\partial c_{ij}/\partial p)_{p=0}$ varies from temperature to temperature. For $(\partial c_{11}/\partial p)_{p=0}$ the experimental error at any temperature was less than 5%. The pressure derivatives of the shear mode constants c_{44} and c' are relatively small and for these derivatives the experimental error is larger. It is estimated as up to 20% at some temperatures. Repeated measurements could not improve on this accuracy.

There are three main features in figure 5. Firstly, of interest, are the very large positive values, between 100 and 200 of $(\partial c_{11}/\partial p)_{p=0}$ in the paramagnetic phase of

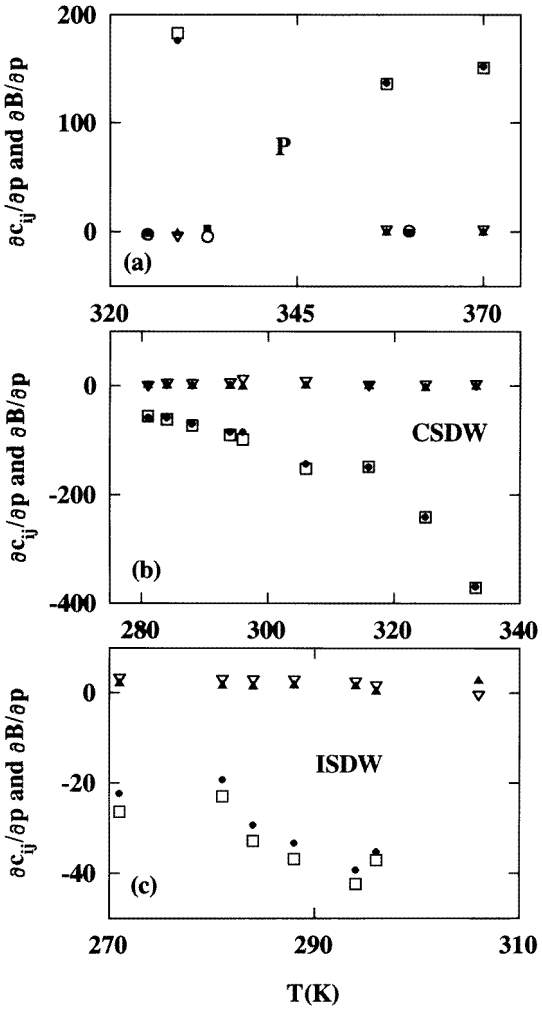

Figure 5. Temperature dependences of the hydrostatic pressure derivatives of the elastic stiffness constants, $(\mathrm{d}c_{ij}/\mathrm{d}p)_{p=0}$, of Cr + 0.07 at.% Ir and Cr + 0.20 at.% Ir. The symbols are: c_{11} (●), c_{44} (▲), c' (▽) and B (□). Panel (*a*) shows the data for the temperature-induced paramagnetic, P, phase of Cr + 0.07 at.% Ir. Also shown in this panel are $(\mathrm{d}c_{44}/\mathrm{d}p)_{p=0}$ (■) and $(\mathrm{d}c'/\mathrm{d}p)_{p=0}$ (○) for the pressure-induced P phase of Cr + 0.02 at.% Ir. Panel (*b*) is for the CSDW phase and panel (*c*) for the pressure-induced ISDW phase of Cr + 0.20 at.% Ir.

Cr + 0.07 at.% Ir when compared to $(\partial c_{11}/\partial p)_{p=0} \approx 10$, observed [11] for paramagnetic Cr + 5 at.% V. Cr + 5 at.% V is usually taken [1] as the reference material to represent the non-magnetic behaviour of antiferromagnetic dilute Cr alloys. The large $(\partial c_{11}/\partial p)_{p=0}$ at $T > T_N$ for Cr + 0.07 at.% Ir indicates large spin-fluctuation contributions to this quantity at $T > T_N$, similarly to what was recently observed in Cr + 3.5 at.% Al [8]. Secondly, $(\partial c_{44}/\partial p)_{p=0}$ and $(\partial c'/\partial p)_{p=0}$ at all temperatures are small, near zero, compared to $(\partial c_{11}/\partial p)_{p=0}$ and $(\partial B/\partial p)_{p=0}$. This observation emphasizes the strong volume dependence of the magnetoelastic interactions in Cr–Ir alloys since c_{44} and c' are associated with volume-conserving strain while c_{11} and B are associated with volume-dependent

strains. Furthermore, measurements at $p = 0$ [7] show only small magnetic anomalies at T_N in c_{44} and c', while large anomalies are observed in c_{11} and B, resulting from a strong volume dependence of the magnetoelastic coupling. The third feature of interest in figure 5 is the large negative $(\partial c_{11}/\partial p)_{p=0}$ and $(\partial B/\partial p)_{p=0}$ in the SDW phases of Cr + 0.20 at.% Ir. Negative $(\partial c_{11}/\partial p)_{p=0}$ and $(\partial B/\partial p)_{p=0}$ were previously also observed in the SDW phases of Cr + 0.3 at.% Ru [3], Cr–Si alloys [9] and in Cr + 3.5 at.% Al [8]. The negative values are unusual as they indicate that c_{11} and B soften under pressure, which is anomalous when compared with the case for normal metals. Furthermore, from figures 5(*b*) and 5(*c*) it is noted that $(\partial c_{11}/\partial p)_{p=0}$ and $(\mathrm{d}B/\mathrm{d}p)_{p=0}$ are more negative in the CSDW phase of Cr + 0.20 at.% Ir than in the ISDW phase. These two quantities are also more strongly temperature dependent in the CSDW than in the ISDW phase of this crystal. The discontinuity in volume ($\Delta V/V \approx 1 \times 10^{-3}$ with $V_{CSDW} > V_{ISDW}$ [7]) at T_{IC} in Cr + 0.20 at.% Ir may partly be responsible for the larger softening of c_{11} and B under pressure in the CSDW phase than in the ISDW phase.

3.3. Grüneisen parameters of the Cr–Ir alloy single crystals

Due to the unusual hysteretic behaviour of $\Delta W/W_0$–p for the Cr + 0.07 at.% Ir crystal in the ISDW phase, we did not calculate the Grüneisen parameters for this crystal at $T < T_N$. They were however calculated for the paramagnetic phase, where near-linear increases in $\Delta W/W_0$ with pressure were observed (figure 1(*b*)).

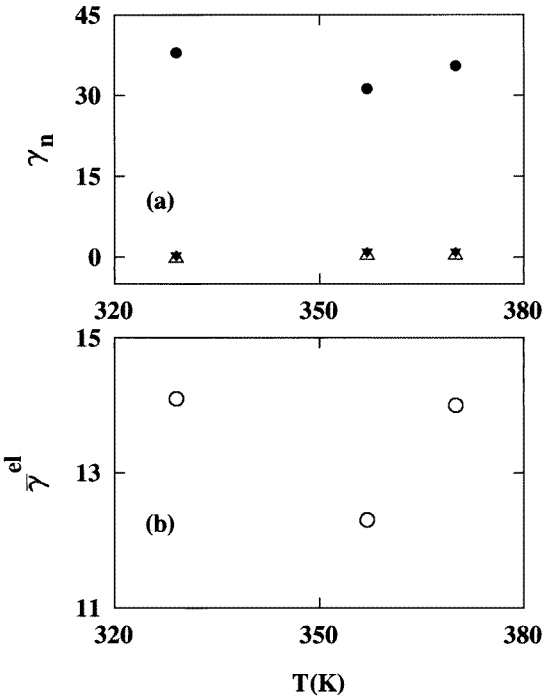

Figure 6. The temperature dependence of the long-wavelength acoustic mode, γ_n, and the mean acoustic, $\bar{\gamma}^{e\ell}$, Grüneisen parameters of Cr + 0.07 at.% Ir in the paramagnetic phase. Panel (*a*) is for [100] wave propagation. The symbols in this panel are: longitudinal mode (●), shear modes (△ and ▼).

The high ultrasonic attenuation at $T > T_N$ for longitudinal mode propagation of the Cr + 0.20 at.% Ir crystal prevents a calculation of the Grüneisen parameters for its P phase. They could however be calculated for the CSDW and ISDW phases of this crystal.

A mode Grüneisen parameter, γ_n, defines the dependence of the acoustic mode frequency, ω_n, in a phonon branch, n, on volume, V, and is expressed as

$$\gamma_n = -\left(\frac{\partial \ln \omega_n}{\partial \ln V}\right)_T \tag{2}$$

which can be obtained from $(\partial c_{ij}/\partial p)_{p=0}$ by using relations given by Brugger and Fritz [12] for the isotropic continuum model. The mean Grüneisen parameter, $\bar{\gamma}^{e\ell}$, which gives the contribution of the acoustic modes at the Brillouin-zone centre to the anharmonicity, is given by

$$\bar{\gamma}^{e\ell} = \left(\sum_{n=1}^{3}\int_{\Omega}\gamma_n \, \mathrm{d}\Omega\right)\Big/\left(3\int_{\Omega}\mathrm{d}\Omega\right).$$

Here the integration is over the whole of space, Ω, and the γ_n are given by equation (2). The procedure for calculating γ_n and $\bar{\gamma}^{e\ell}$ from $(\partial c_{ij}/\partial p)_{p=0}$ was discussed in detail previously [3, 8]. The temperature dependences of γ_n, along the fourfold [100] axis, and $\bar{\gamma}^{e\ell}$ for Cr + 0.07 at.% Ir at $T > T_N$ are shown in figure 6.

Figure 7 shows the temperature dependence of γ_n for the Cr + 0.20 at.% Ir crystal along the [100] axis as well as that for $\bar{\gamma}^{e\ell}$. Figures 7(*a*) and 7(*c*) are for the CSDW phase below

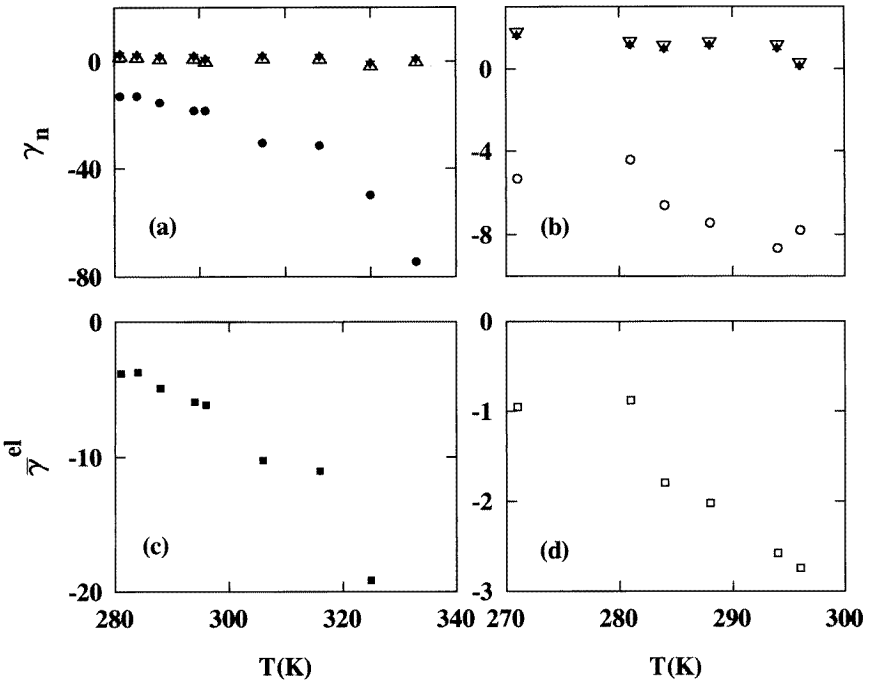

Figure 7. Temperature dependences of the long-wavelength acoustic mode Grüneisen parameters, γ_n, for [100] wave propagation and the mean acoustic, $\bar{\gamma}^{e\ell}$, Grüneisen parameter for Cr + 0.20 at.% Ir. Panels (*a*) and (*c*) are for the CSDW phase and panels (*b*) and (*d*) for the pressure-induced ISDW phase. The symbols in panels (*a*) and (*b*) are: longitudinal mode γ_n: ● and ○, respectively, and shear mode γ_n: ▼ and △ in panel (*a*) and ▲ and ▽ in panel (*b*).

p_{IC} and figures 7(*b*) and 7(*d*) for the pressure-induced ($p > p_{IC}$) ISDW phase.

The long-wavelength acoustic mode Grüneisen parameters γ_n, are plotted in figure 8 as a function of mode propagation direction for both the ISDW and CSDW phases of Cr + 0.20 at.% Ir at 296 K, as typical examples. The anisotropy effects are relatively small (figure 8) in both the ISDW and CSDW phases of this crystal at all temperatures studied.

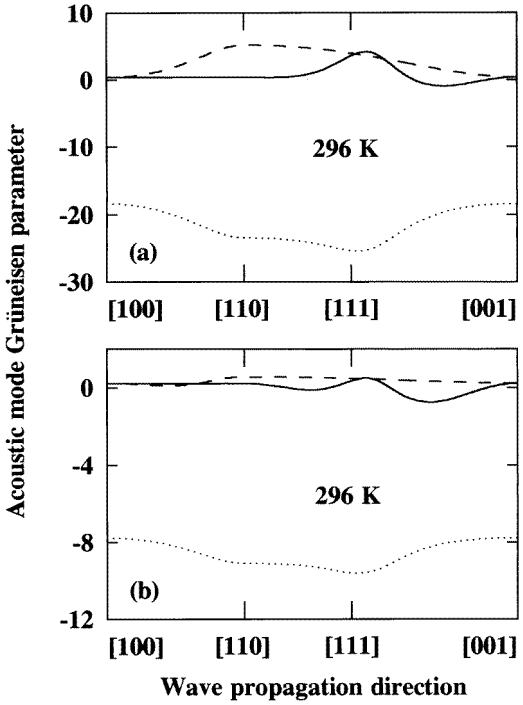

Figure 8. Long-wavelength longitudinal (dotted lines) and shear (solid and dashed lines) acoustic mode Grüneisen parameters of Cr + 0.20 at.% Ir as functions of the mode propagation direction in the CSDW (panel (*a*)) and the pressure-induced ISDW (panel (*b*)) phases at 296 K.

4. Summary and conclusions

The main features of the present study on the two Cr–Ir alloy single crystals are summarized as follows:

(1) The longitudinal mode ultrasonic wave velocity of Cr + 0.07 at.% Ir behaves hysteretically under increasing and decreasing applied hydrostatic pressures in the ISDW phase at temperatures $T < T_N$. Similar behaviour was recently [9] also observed in an ISDW Cr + 0.5 at.% Si single crystal. The concentrations of both of these crystals are below the triple-point concentration on the magnetic phase diagram. In both of them, the longitudinal wave velocity is only slightly pressure dependent in the ISDW phase. This is in contrast with the relatively large pressure dependence of this velocity in the pressure-induced ISDW phase of the Cr + 0.20 at.% Ir crystal, as represented by the large negative dc_{11}/dp of figure 5(*c*). In the paramagnetic phases at $T > T_N$ of both Cr + 0.07 at.% Ir and Cr + 0.5 at.% Si alloys, the longitudinal wave velocity, on

the other hand, shows a very large, nearly linear, pressure dependence (figure 1). The acoustic mode Grüneisen parameter for longitudinal mode propagation along [100] of Cr + 0.07 at.% Ir in the paramagnetic phase (figure 6) is $\gamma_n \approx +35$ (roughly constant in the temperature range 329 K to 370 K of the measurements), which is very similar to the value for Cr+0.5 at.% Si at T just above T_N. In both these crystals this value is however about 15 times that ($\gamma_n = +2.25$) observed [11] at room temperature for paramagnetic Cr+5 at.% V. The γ_n for the shear mode at $T > T_N$ for all three of the above crystals are roughly of the same magnitude, and for the Cr+0.07 at.% Ir and Cr+0.5 at.% Si crystals they are much smaller (nearly 40 times smaller for Cr+0.07 at.% Ir (figure 6)) than the γ_n for the longitudinal mode. $\bar{\gamma}^{e\ell}$ for the paramagnetic phase of the Cr+0.07 at.% Ir crystal is roughly ten times that for paramagnetic Cr+5 at.% V [11]. This behaviour is attributed to strong coupling of longitudinal phonons to spin fluctuations in Cr + 0.07 at.% Ir.

(2) The large negative longitudinal mode Grüneisen parameters for the SDW phases of Cr + 0.20 at.% Ir, compared to the small positive values observed [11] for paramagnetic Cr + 5 at.% V, show strong magnetoelastic coupling between the long-wavelength longitudinal phonons and the SDW in Cr + 0.20 at.% Ir. The shear mode Grüneisen parameters of this crystal are small and positive, very similar to that obtained [11] for Cr + 5 at.% V, showing that shear mode interactions are relatively weak. Similar effects were recently [3] observed in a Cr + 0.3 at.% Ru crystal.

(3) The Grüneisen parameters for the CSDW phase of Cr + 0.20 at.% Ir are more negative and more temperature dependent than in the ISDW phase. This indicates stronger magnetoelastic interaction in the CSDW phase than in the ISDW phase of Cr + 0.20 at.% Ir, similarly to what was observed for a Cr + 0.3 at.% Ru [3] sample. As the temperature is increased toward the Néel point, the longitudinal mode softening in the CSDW phase of both of these crystals becomes greatly enhanced.

(4) The mean acoustic Grüneisen parameters for the CSDW and ISDW phases of Cr + 0.20 at.% Ir are nearly the same as those for the same phases of Cr + 0.3 at.% Ru [3]. For instance, for both, $\bar{\gamma}^{e\ell} \approx -20$ for the CSDW phase at 50 K below the Néel temperature of each. The magnetoelastic interactions in these two systems of alloys of Cr with group-8 non-magnetic transition metals seem therefore to be of roughly equal strength.

(5) The long-wavelength acoustic mode Grüneisen parameter of Cr + 0.20 at.% Ir is only slightly anisotropic at all temperatures studied, both in the ISDW and CSDW phases. This is also the case for Cr + 0.3 at.% Ir [3], meaning that the interaction of the SDW with the acoustic longitudinal phonons is effectively isotropic in both of them.

In conclusion, the role of magnetoelastic effects in the acoustic mode vibrational anharmonicity has been studied near the ISDW–CSDW/CSDW–ISDW phase transitions of Cr + 0.20 at.% Ir as well as for the P phase of Cr + 0.07 at.% Ir. The anharmonicity through the ISDW–CSDW/CSDW–ISDW phase transitions of Cr + 0.20 at.% Ir behaves very similarly to that recently observed for Cr + 0.3 at.% Ru. The latter alloy is also one of the group of alloys of Cr with group-8 non-magnetic transition metals and is the only Cr alloy that has been studied up to now looking for anharmonic effects through an ISDW–CSDW/CSDW–ISDW transition. It has now been established that the observation of large negative Grüneisen parameters and larger magnetoelastic interactions in the CSDW phases than in the ISDW phases are more general phenomena for these types of alloy. The present study confirms that the strong magnetoelastic coupling at the ISDW–CSDW/CSDW–ISDW transitions in alloys of Cr with group-8 non-magnetic transition metals takes place mainly with the volume strain. This strong volume dependence is currently not understood properly

on a theoretical basis. It was suggested [2] that the strong volume dependence is not to be sought in the nesting property of the Fermi surface of the Cr alloys, but that it should be sought in theories that take lattice strain energy into account.

The question of the strong volume dependence of the properties of Cr was recently addressed by Marcus, Qiu and Moruzzi [13]. They showed that two properties of Cr are to be used to explain its antiferromagnetism. One is the nesting effect of the electron and hole Fermi surface sheets and the other is a new special property, arising from total-energy calculations for bcc Cr. These calculations show that, although the lowest energy state is non-magnetic, a small expansion of the lattice induces an antiferromagnetic state. The strong volume dependence of the properties of Cr is physically explained by combining the above two properties. This theory however does not attempt to explain the strong volume dependence of the magnetoelastic interactions and acoustic mode vibrational anharmonicity in dilute Cr alloys.

Acknowledgment

Financial aid from the South African Foundation for Research Development is acknowledged.

References

[1] For a comprehensive review on the magnetic properties of Cr alloys, see
Fawcett E, Alberts H L, Galkin V Yu, Noakes D R and Yakhmi J V 1994 *Rev. Mod. Phys.* **66** 25
[2] Fawcett E 1997 *Physica* B **239** 71
[3] Cankurtaran M, Saunders G A, Wang Q, Ford P J and Alberts H L 1992 *Phys. Rev.* B **46** 14 370
[4] Mañosa Ll, Saunders G A, Rahdi H, Kawald U, Pelzl J and Bach H 1991 *J. Phys.: Condens. Matter* **3** 2273
[5] Sidov V A and Khostantsev L G 1994 *J. Magn. Magn. Mater.* **129** 356
[6] Iwai J, Miyai N, Kizaki T and Kim D J 1995 *J. Magn. Magn. Mater.* **140–144** 243
[7] Martynova J, Alberts H L and Smit P 1997 *J. Phys.: Condens. Matter* **9** 3461
[8] Alberts H L and Smit P 1995 *Phys. Rev.* B **51** 15146
[9] Prinsloo A R E, Alberts H L and Smit P 1997 *Phys. Rev.* B **56** 11 777
[10] Thurston R N 1965 *Proc. IEEE* **53** 1320
[11] Cankurtaran M, Saunders G A, Wang Q and Alberts H L 1996 *Phil. Mag.* B **74** 349
[12] Brugger K and Fritz T C 1967 *Phys. Rev.* **157** 524
[13] Marcus P M, Qiu S-L and Moruzzi J 1998 *J. Phys.: Condens. Matter* **10** 6541